

**A Preliminary Report on L2C Data Collection and Analysis
using a Trimble R7 GPS Receiver**

Liliána Sükeová

Marcelo C. Santos

Richard B. Langley

Rodrigo F. Leandro

*Geodetic Research Laboratory
Department of Geodesy and Geomatics Engineering
University of New Brunswick
P. O. Box 4400
Fredericton, NB, Canada
E3B 5A3*

20 January 2007

1. Introduction

The United States started an extensive modernization program to provide better service to Global Positioning System (GPS) users. This modernization program includes launching of modernized GPS satellites such as the recently launched SVN 53, for which the PRN 17 was assigned. The block of these new satellites is called Block IIR-M, where “R” stands for replenishment and “M” for modernized. In this modernization process the GPS has gained a new open civil signal (called L2C), centered at the L2 frequency. The first modernized satellite, PRN 17, was launched on 25 September 2005 and the new L2C signal is fully available from 15 December 2005. The third frequency band L5 (centered at 1176.55 MHz) will arrive with the Block IIF (“F” – Follow on) satellites, now scheduled to start to be launched in 2008.

From the time the PRN17 is in orbit, the L2C signal has become an issue of worldwide interest to the GPS research communities. Enhanced receivers capable of tracking the modernized GPS signal have been developed and provided by a number of manufacturers, such as Trimble Navigation Ltd. IGS (International GNSS Service) has organized a network of L2C signal tracking stations which have been established in different places in the world.

The Canadian distributor of Trimble Navigation Ltd. is Cansel. Cansel loaned to the University of New Brunswick (UNB) Fredericton, Department of Geodesy and Geomatics Engineering (GGE) a Trimble R7 receiver, which is capable of tracking the

L2C signal. The receiver was connected to the same antenna used by IGS station UNB1 (now UNBJ) and has become a part of the L2C signal tracking network.

In this paper a description of the L2C data collection using the Trimble R7 receiver is made; however the major focus will be on the L2C signal analysis.

2. Objectives of the project

The general objective of the investigation reported in this project is:

- to analyze the L2C signal, which is currently transmitted by modernized IIR–M satellite PRN 17.

The specific objectives of the investigation are:

- to establish a station using Trimble R7 receiver,
- to collect the data containing the new L2C observations,
- to test the receiver's firmware.

3. Project description

3.1 The L2C tracking station

As previously mentioned, the Trimble R7 receiver has been on loan to GGE/UNB from the middle of December 2005 to date. After initial testing procedures the receiver was connected to the same antenna used by former IGS station UNB1 (currently UNBJ), by means of an antenna splitter. The Trimble R7 was called UNB3 and has become one

of the L2C signal tracking stations. The network of L2C signal tracking stations as of the 11 January 2006 is illustrated in Figure 3.1, including UNB3.

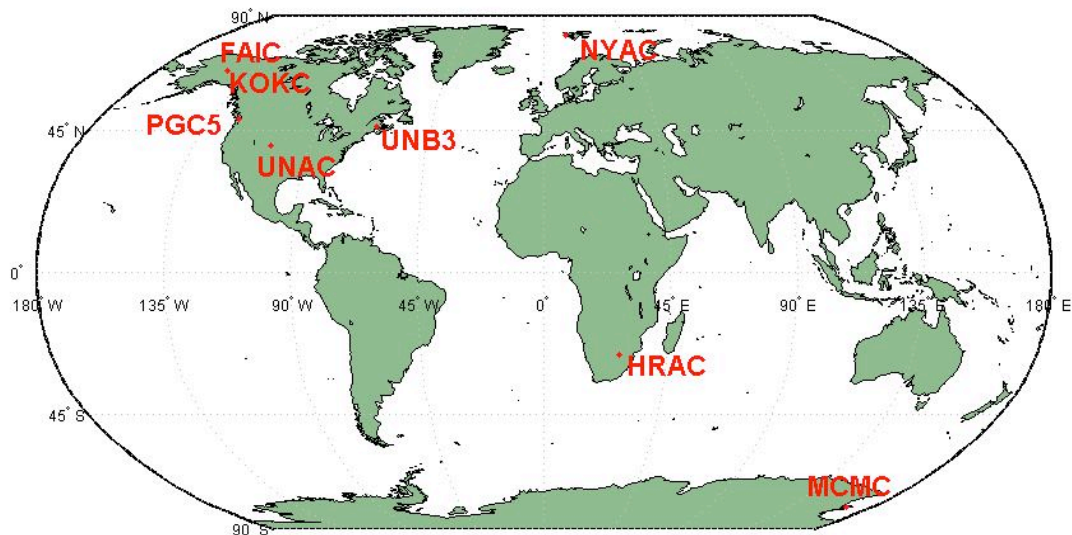


Figure 3.1 L2C tracking network

3.2 Technical specifications of UNB3

This section summarizes the site identification of the monument, the site location information, information about the receiver and antenna, following the usual IGS site information format (Tables 3.1 to 3.4). Tables 3.1 to 3.4 are effective until 15 August 2006.

Table 3.1 Site Identification of the GNSS Monument

Site Name	Four Character ID	Monument Inscription IERS DOMES Number	Additional Information :
University of New Brunswick, Fredericton	UNB3	50156S001	UNB3 is using UNB1's antenna (via splitter) Mast is fixed to penthouse wall on top of Head Hall, UNB, Fredericton

Table 3.2 Site Location Information

City or Town	State or Province	Country	Tectonic Plate
Fredericton	New Brunswick	Canada	North American

Table 3.3 GNSS receiver information:

Name	Serial number	Firmware version	Satellite System
Trimble R7	0220330315	NP 2.26 / SP 2.26	GPS

Table 3.4 GNSS antenna information

Name	Serial Number
JPSREGANT_DD_E	RA0193

3.3 Changes in the site information documentation and in receiver firmware

As a result of the need to install a new adapter on the mast supporting the UNB1 antenna, the IGS has decided that UNB1 (DOMES No. 50156S001) should be

decommissioned. For UNB1, there was no marker and all position determinations referred to the Antenna Reference Point (ARP) = Bottom of Preamplifier (BPA). The new adapter was installed on 16 August 2006.

A new DOMES number (50156M002) and 4-letter station ID (UNBJ) have been established. The new DOMES number and station ID refer to a "marker" which is at the top of the mast where it connects with the antenna adapter, on the mast's axis. The ARP = BPA is 0.3001 m above the marker. The position of the UNBJ ARP is approximately 0.227 m above UNB1's ARP (Langley, 2006).

In order to be consistent with the changes of the IGS station UNB1, it was necessary to introduce additional information for UNB3 in the header of its observation RINEX files. Also, since UNB3 still uses UNB1 (former IGS site) coordinates, a height offset of 0.227m was introduced and additional comments were added for UNB3, such as:

- ARP coincides with (IGS site) UNBJ's ARP.
- Site coordinates coincide with (former IGS site) UNB1's ARP.
- For UNB1/UNBJ relation refer to IGSMAIL-5406.

Marker information was also changed to:

- Marker name: UNB3 (using UNBJ's antenna).

The firmware of the Trimble R7 receiver was upgraded on 18 August 2006 from version 2.26 to version 2.28. Even though the version 2.30 (which was released on 21 September 2006) is the latest firmware version since v.2.28 it has not been used during the data collection.

4. Observations and their analysis

4.1 Data collection

The data collection using Trimble R7 receiver began on 11 January 2006 and ended on 10 October 2006. The 30 second daily RINEX files containing the new L2C measurements have been uploaded to the ftp server of the Crustal Dynamics Data Information System (CDDIS) at NASA's Goddard Space Flight Center: <ftp://cddis.gsfc.nasa.gov/gps/data/l2ctest/daily/2006/>, where data from all stations in the IGS L2C network can be found.

4.2 Data processing

In order to accommodate the new GPS L2C pseudorange observable a new observable code (C2) has been created to be used in RINEX (v. 2.11) observation files. The daily observation and navigation files have been created using program TEQC, version 5 November 2005, which can be freely obtained from the University NAVSTAR Consortium (UNAVCO) web page (<http://www.unavco.org/>). While translating raw data binary files to RINEX files using TEQC, an additional flag (+C2) has to be used at the beginning of the command line to enable the L2C data to be displayed in the observation files. The full command line reads:

```
teqc +C2 -tr d +nav *.06n *.dat > *.06o
```

After being created, RINEX observation files have been compressed to Hatanaka format (compact RINEX format) using the conversion software RNX2CRX, which can be freely obtained from Geographical Survey Institute (Japan) ftp server at <ftp://terras.gsi.go.jp/software/RNXCMP/>. As a result of this compression, we get original GPS observations in a smaller ASCII file (*.06d). The acquired navigation and Hatanaka files have been uploaded to the CDDIS ftp server daily and are available as indicated above.

All the programs were run under Windows XP Professional version 2002 on a Dell OptiPlex GX620 computer. Trimble software facilities have been used for receiver setup and monitoring, such as the GPS Configurator, which has been used for monitoring purposes and receiver setup. The software is provided by Trimble and is used to view the current receiver settings, change receiver settings and check GPS information (information about the antenna, about the receiver's firmware and hardware, general logging settings, information about receiver's current position, and information about the satellites the receiver is tracking).

The collected data has been saved on the receiver's flash card and transferred to the monitoring computer by using Trimble Data Transfer.

4.3 Observed data

The UNB3 RINEX files contain the following observables: C1, C2, P2, L1, L2, S1 and S2. C1 stands for C/A code, C2 for L2C code, P2 for P2(Y) code measurements, L1 and L2 for carrier-phase measurements on the L1 and L2 frequencies, respectively, and

S1 and S2 are the signal-to-noise ratio (SNR) for each satellite. A new observable column was introduced to accommodate L2C observations (C2's column); however this column is populated only for IIR-M satellites (such as PRN17), and there are no P2 observations for these satellites. In the case of satellites of other blocks, C2 column remains empty and P2 column is filled with P2 code observations.

SNR values on the L1 and L2 frequencies for all satellites are illustrated in Figures 4.1 and 4.2, respectively. The values are referring to day: 16 January 2006. The range of the SNR values on the L1 frequency (Figure 4.1) is approximately 29.5 to 54 dB-Hz for all satellites, while the range of the SNR values on the L2 frequency (Figure 4.2) is approximately 14 to 45 dB-Hz for all satellites except PRN 17. By comparing the SNR levels on each frequency it is clear that the SNR of PRN 17 on L2 is higher than those for all other satellites. This indicates an improvement of L2C signal's SNR over the P(Y) code.

The SNR of PRN17 on both frequencies is plotted in Figure 4.3. We can see that the values on each frequency are almost overlapping each other. Figure 4.4 shows that the SNR of another satellite (PRN 11) on P2 code measurements is lower than on the C/A observations. The maximum elevation angles of PRN 17 and PRN 11 are 80 and 70 degrees, respectively.

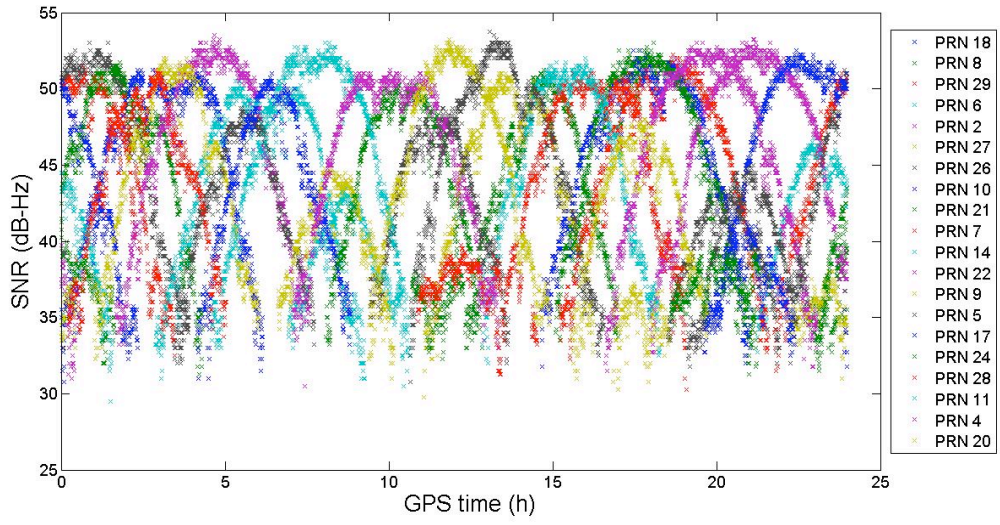


Figure 4.1 Signal-to-noise ratio on L1

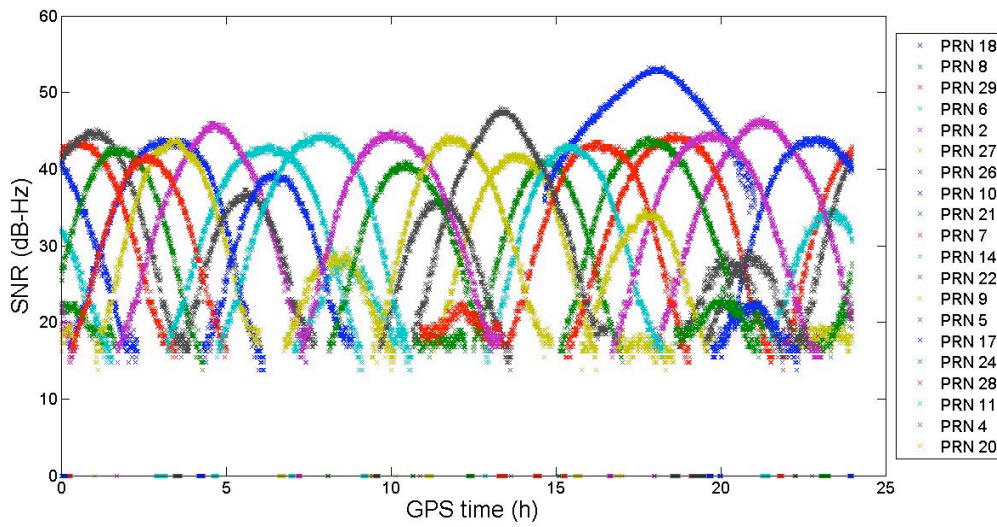


Figure 4.2 Signal-to-noise ratio on L2

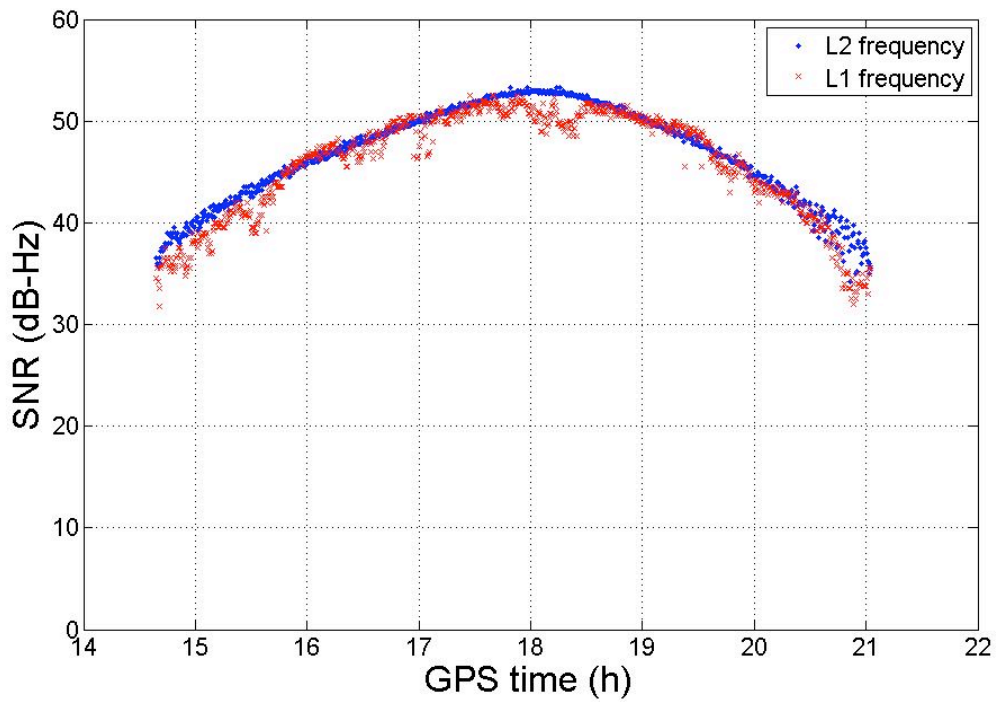


Figure 4.3 SNR of PRN 17 on L1 and L2

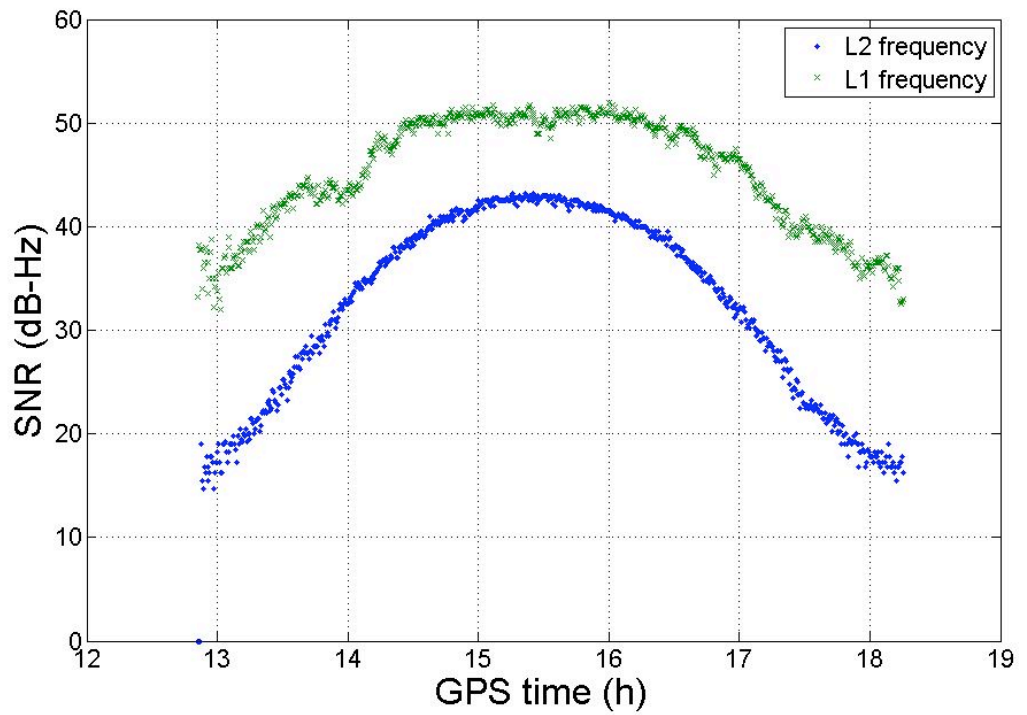


Figure 4.4 SNR on L1 and L2 PRN 11

4.4 L1 and L2 pseudoranges and their analyses

In order to make a comparison between pseudoranges measured on the two frequencies, the differences between the measured pseudoranges on L1 (C/A) and L2 (L2C) for PRN 17 were calculated (in the sense of C2-C1) for day 16 January 2006. Figure 4.5 shows the results of this operation. The range of the differences reaches approximately 5 m at low elevation angle and approximately 2.5 m at higher elevation angles. As expected, the spread of the differences is lower in higher elevation angle and higher in low elevation angle, which is a direct effect of the relation between measurement noise level and elevation angle. The period of observation of the illustrated differences is approximately 6.5 hours. Figure 4.6 shows the similar results for PRN 11. We can see that the differences have similar distribution.

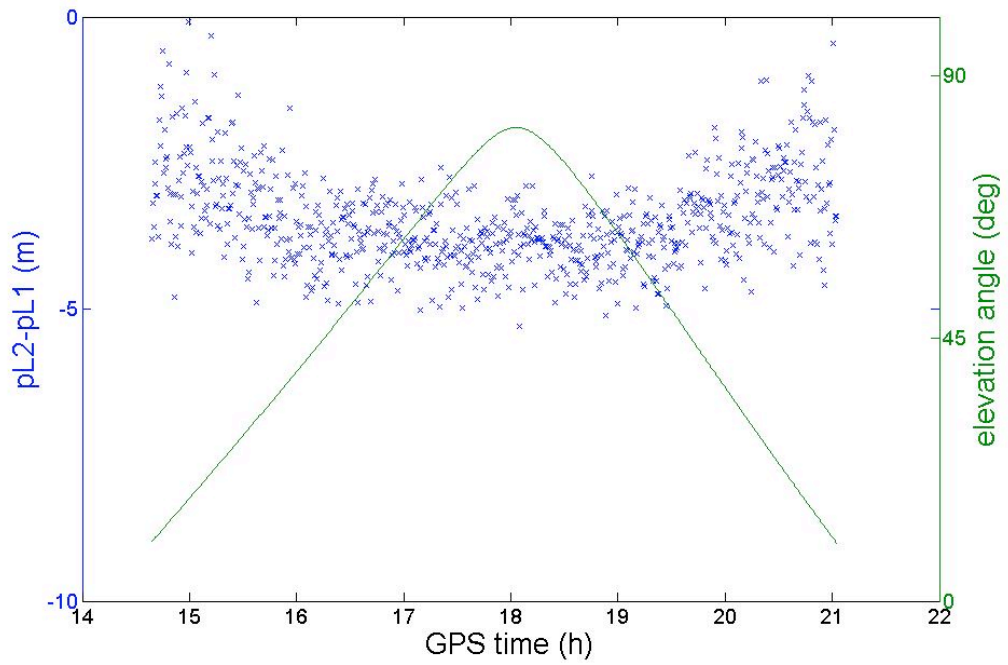


Figure 4.5 Variation of the differences between the pseudorange measurements on L1 and L2 (blue crosses), and elevation angle (green line) for PRN 17

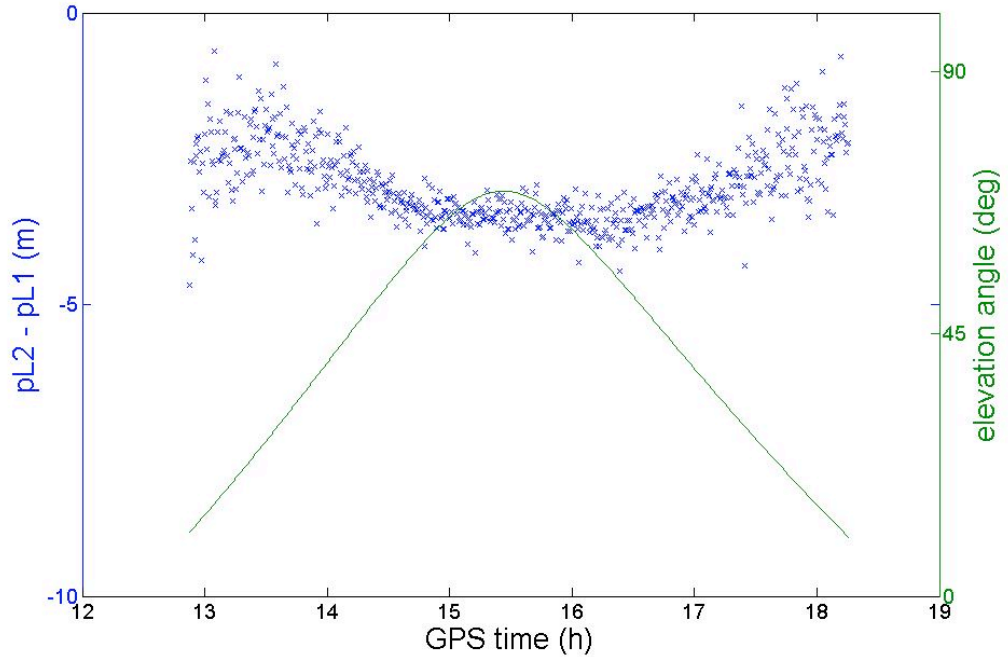


Figure 4.6 Variation of the difference between the pseudorange measurements on L1 and L2 (blue crosses) and elevation angle (green line) for PRN 11

The linear combination used in this analysis ($\text{pseudorange}_{L2} - \text{pseudorange}_{L1}$) is the “geometry free linear combination”, which completely eliminates the geometric terms and associated errors (satellite orbit, clock offsets, and troposphere). The remaining difference shown in the plotted data (figures 4.5 and 4.6) is mainly due to the differential code biases (DCB), the ionospheric refraction varying over time with respect to the elevation angle of the satellite, multipath and code noise.

In order to demonstrate that the Figures 4.5 and 4.6 are consistent with the variation of the ionospheric refraction on 16 January 2006, the differences between the measured pseudoranges on L1 and L2 frequencies for stations UNB1 and UNB3 were calculated and compared. The measured pseudoranges refer to the same satellite PRN17 for both stations. As the Javad receiver used by the IGS station UNB1 does not track the L2C signal, the difference for UNB1 was calculated using C/A and P2 code pseudoranges.

Subtracting the mean of the computed differences for both stations allows us to better comparison of the two results. The computed differences with their mean removed are illustrated in Figure 4.7. The diverse scatter of the two plots is due to different noise of L2C and P2 codes. Consequently the remaining effects causing the variation of the differences are the variation of the ionospheric refraction and multipath. From Figure 4.7 we can clearly see that these effects (the variation of the ionospheric refraction and multipath) are consistent for both stations UNB3 and UNB1. Since two different receivers were used and the variation of the code differences over time is consistent between them, we can also conclude that, for the most part, the receiver-dependent differential code biases were eliminated with the reduction of the mean, which means the receiver DCB's could probably be considered as (nearly) constant over these six

hours of observation. Therefore the variation over time of the illustrated difference between L1 and L2 pseudoranges (Figures 4.5, 4.6 and 4.7) can be considered mainly due to the variation of the ionospheric refraction, multipath and code noise.

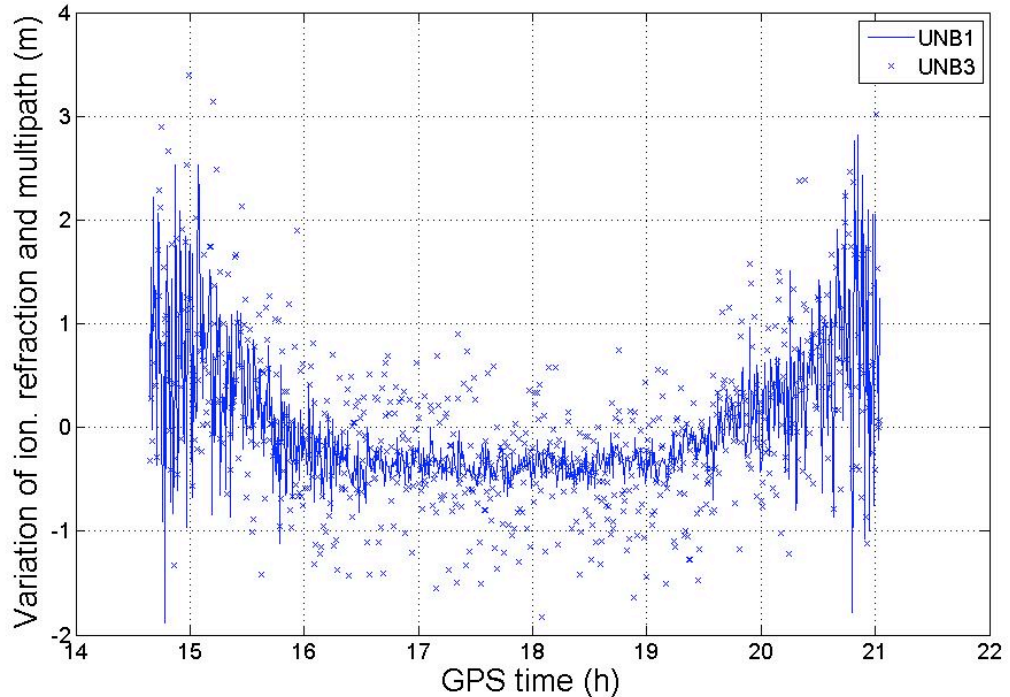


Figure 4.7 Variation of the ionospheric refraction and multipath on PRN17 for stations UNB1 and UNB3

According to Figure 4.8 obtained from Space Environment Center (2006), the largest planetary geomagnetic index (Kp-index) for the day 16 January 2006 was 4. As the Kp-index scale has a range from 0 to 9, it indicates that there was no significant disturbance in the Earth's magnetic field on this particular day.

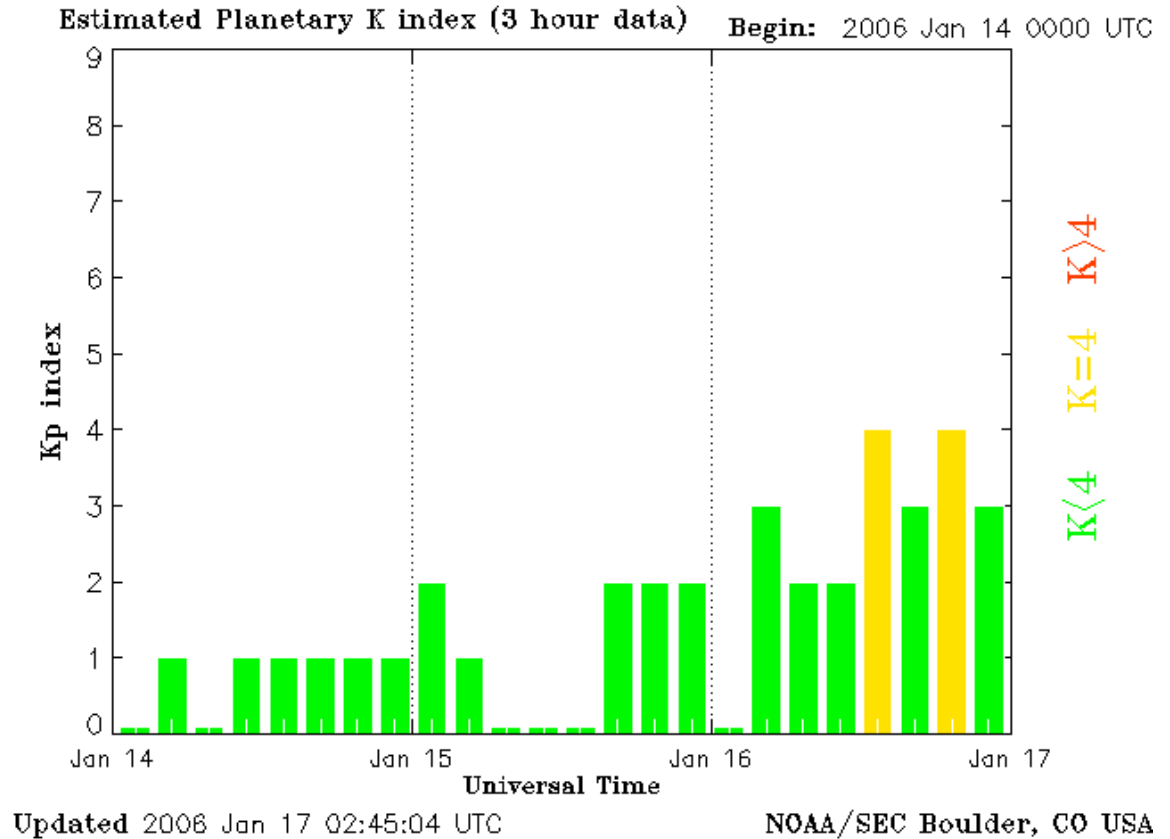


Figure 4.8 Estimated planetary K index (Kp-index) from 14 to 16 January 2006

5. Noise level of the signal

The objective of this section is to analyze the multipath and noise level of C/A and L2C code pseudoranges for PRN 17, as compared to the noise and multipath level of P2 and C/A code for PRN 11.

5.1 Code multipath and noise level estimation procedure

An observable which only contains receiver noise and multipath effects was created by differencing the raw pseudorange measurement, given by equation (5.1), and the raw carrier-phase measurement, given by equation (5.2), both of them with their ionospheric

delay removed. This procedure follows the steps given by Langley (1998). This section will explain how to remove the ionospheric delay from the raw carrier-phase and pseudorange observations, and how to obtain the code noise and multipath.

At first, we will look at the pseudorange and carrier-phase measurement simplified equations, which are both expressed in length units.

The pseudorange measurement equation:

$$p_i = \rho + c(dT - dt) + d_{ion_i} + d_{trop} + mp_{p_i} + \varepsilon_{p_i}, \quad (5.1)$$

And the carrier-phase measurement equations:

$$\Phi_i = \rho + c(dT - dt) + \lambda_i N_i - d_{ion_i} + d_{trop} + mp_{\Phi_i} + \varepsilon_{\Phi_i}. \quad (5.2)$$

In equation (5.1) i stands for the L1 or L2 frequency, p_i is the measured pseudorange on the L1 or L2 frequency, ρ is the actual geometric distance between the receiver and satellite antennas, dT and dt are the receiver and the satellite clock offsets relative to GPS Time (GPST), respectively, d_{ion_i} and d_{trop} are the ionospheric and tropospheric propagation delays, respectively, mp represents the effect of multipath and ε the noise term.

In equation (5.2) λ_i is the wave length of the signal and N_i represents the carrier-phase ambiguity. The other terms in the carrier-phase observations equation stand for the

same effects as in the pseudorange observation equation (5.1) explained above. Other terms such as satellite and receiver equipment biases have been ignored.

The ionospheric delay, which later will be removed from both pseudorange and carrier-phase measurements, can be expressed as follows:

$$d_{ion_2} = d_{ion_1} \frac{f_1^2}{f_2^2}, \quad (5.3)$$

where f_1 and f_2 are the carrier frequencies on L1 and L2. By forming the difference between the carrier-phase measurements on L1 and L2, the ionospheric delay on L1 can be computed with an additive constant (mainly caused by ambiguities) and with multipath and noise contributions as:

$$\Phi_2 - \Phi_1 = d_{ion_1} - d_{ion_2} + \lambda_2 N_2 - \lambda_1 N_1 + mp_{\Phi_2} - mp_{\Phi_1} + \varepsilon_{\Phi_2} - \varepsilon_{\Phi_1}. \quad (5.4)$$

Solving for d_{ion_1} gives:

$$d_{ion_1} = \left(\frac{f_2^2}{f_1^2 - f_2^2} \right) (\Phi_1 - \Phi_2 + \lambda_2 N_2 - \lambda_1 N_1 + mp_{\Phi_2} - mp_{\Phi_1} + \varepsilon_{\Phi_2} - \varepsilon_{\Phi_1}). \quad (5.5)$$

The measure of the L1 ionospheric delay could be used to correct both code and carrier-phase measurements, if we knew carrier-phase multipath and noise values and the integer ambiguities. At best, we can compute a relative ionospheric delay d^* which

includes a constant contribution from the integer carrier-phase ambiguities, the multipath and noise terms (Langley, 1998):

$$d_{ion_1}^* = \left(\frac{f_2^2}{f_1^2 - f_2^2} \right) (\Phi_1 - \Phi_2). \quad (5.6)$$

Although the estimate of the ionospheric delay from carrier-phase measurements is biased by the ambiguities, when we use it to correct carrier-phase and pseudorange observations (by removing the relative ionospheric delay from both measurements) and difference the result we get (Langley, 1998):

$$\begin{aligned} & \left[p_1 - \left(\frac{f_2^2}{f_1^2 - f_2^2} \right) (\Phi_1 - \Phi_2) \right] - \left[\Phi_1 + \left(\frac{f_2^2}{f_1^2 - f_2^2} \right) (\Phi_1 - \Phi_2) \right] = \\ & p_1 - \left(\frac{f_1^2 + f_2^2}{f_1^2 - f_2^2} \right) \Phi_1 + \left(\frac{2f_2^2}{f_1^2 - f_2^2} \right) \Phi_2. \end{aligned} \quad (5.7)$$

If we assume, that the geometric distance, ρ , the receiver clock offset dT ; and the satellite clock offset, dt , are the same for L1 and L2 carrier phase and pseudorange measurements, we arrive at the following equation:

$$\begin{aligned}
p_1 - \left(\frac{f_1^2 + f_2^2}{f_1^2 - f_2^2} \right) \Phi_1 + \left(\frac{2f_2^2}{f_1^2 - f_2^2} \right) \Phi_2 &= mp_{p_1} + noise_{p_1} \\
- \left(\frac{f_1^2 + f_2^2}{f_1^2 - f_2^2} \right) (\lambda_1 N_1 + mp_{\Phi_1} + noise_{\Phi_1}) & \\
+ \left(\frac{2f_2^2}{f_1^2 - f_2^2} \right) (\lambda_2 N_2 + mp_{\Phi_2} + noise_{\Phi_2}). &
\end{aligned} \tag{5.8}$$

The right-hand side of the equation (5.8) contains the pseudorange and carrier-phase multipath and noise and the ambiguity term. Since the carrier-phase measurement multipath and noise is insignificant in comparison with code multipath and noise, the right-hand side of the equation (5.8) gives the multipath and noise of the code measurement, offset by a constant component due to the carrier-phase ambiguities.

5.2 Code multipath and noise level analysis

In this section the multipath and noise level of C/A and L2C codes for PRN 17 and PRN 11 are analyzed. The noise plus multipath values referred to frequencies L1 and L2 were computed using the approach described above. In order to better illustrate the noise level and the multipath, the mean of the computed values were removed. The results for 16 January 2006 are illustrated in Figures 5.2 and 5.4 for PRN 17 and PRN 11, respectively.

Similarly, the above described steps can be used to calculate the multipath and noise of the L2C and P2 codes, by taking into account that the ionospheric delay on L2 is different from that on L1 (see equation (5.3)). The resulting multipath and noise levels for L2C (PRN 17) and P2 codes (PRN 11) are illustrated in Figures 5.1 and 5.3,

respectively, with their mean value removed. The standard deviations of C/A, L2C and P2 code multipath and noise levels are summarized in Tables 5.1 and 5.2. The elevation angles of the satellites PRN 17 and PRN 11 are plotted in Figures 3.5 and 3.6, respectively.

From Tables 5.1 and 5.2, we can see that the C/A-code noise level of PRN 17 is slightly smaller than for PRN 11. This difference is expected because PRN 17 is observed at slightly higher elevation angles compared to PRN 11. Even though one might expect to see also smaller noise levels for L2C from PRN 17 compared to P2 from PRN 11, it can be noticed that the L2C noise level for PRN 17 is actually higher than for P2, as observed for PRN 11. The causes of this behavior are discussed in the next section.

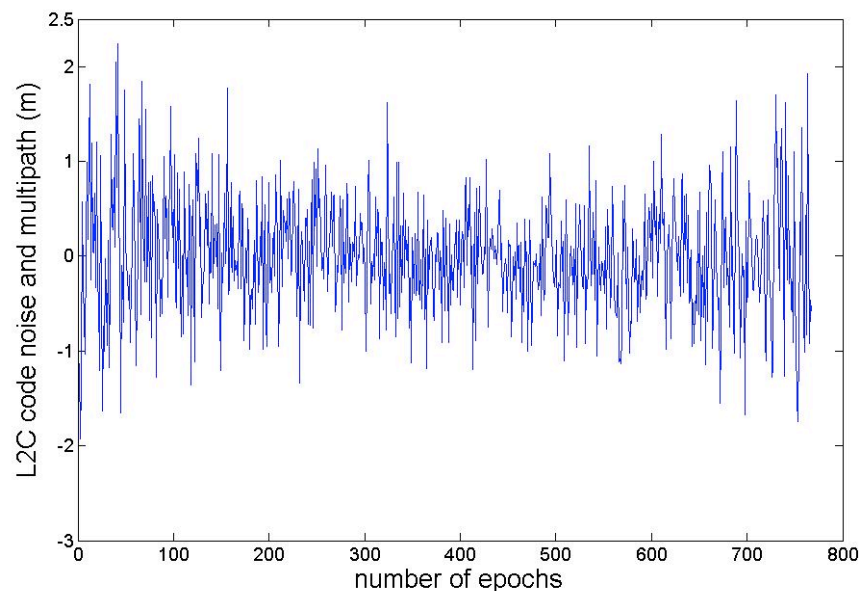


Figure 5.1 Noise and multipath level of L2C – PRN 17

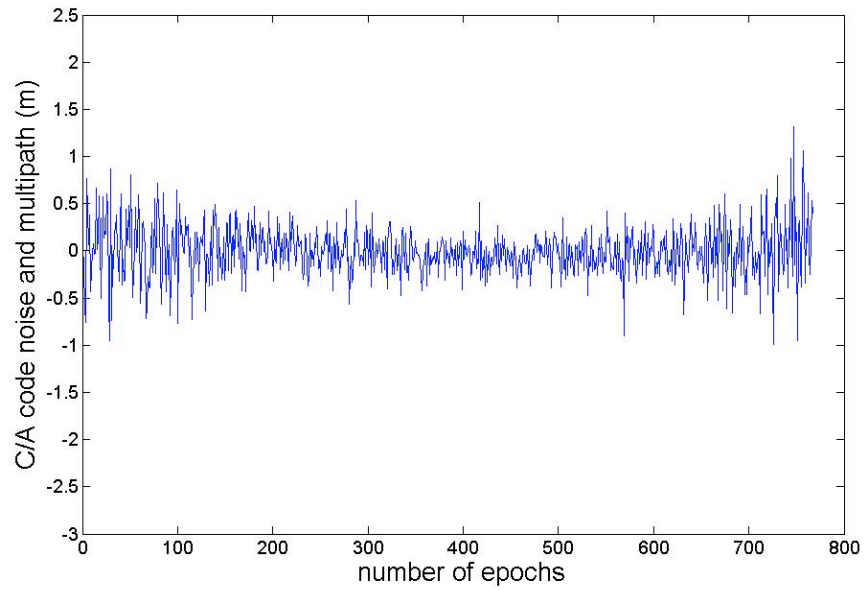


Figure 5.2 Noise and multipath level of C/A code – PRN 17

Table 5.1 Standard deviation of L2C and C/A-code noise and multipath – PRN 17

	Standard deviation (m)
L2C	0.611
C/A	0.270

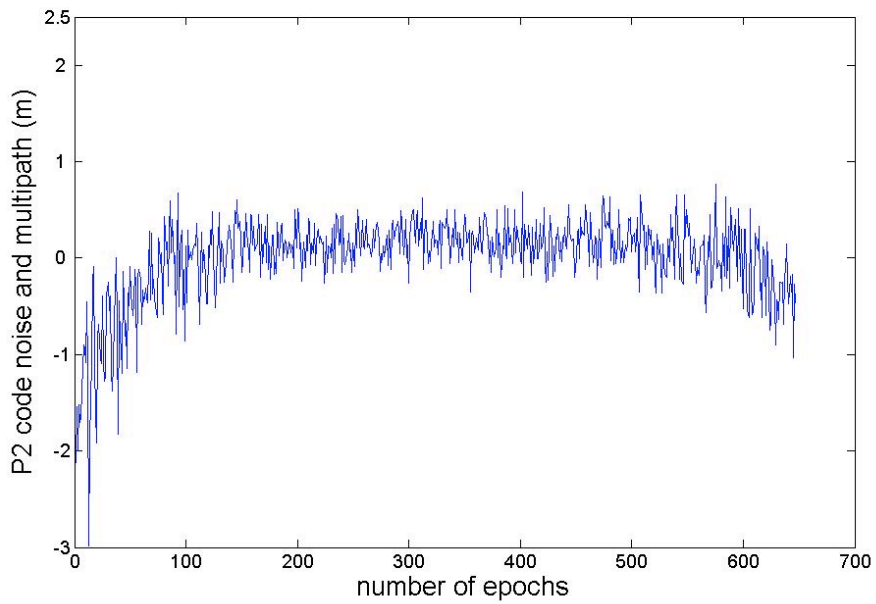


Figure 5.3 Noise and multipath level of P2– PRN 11

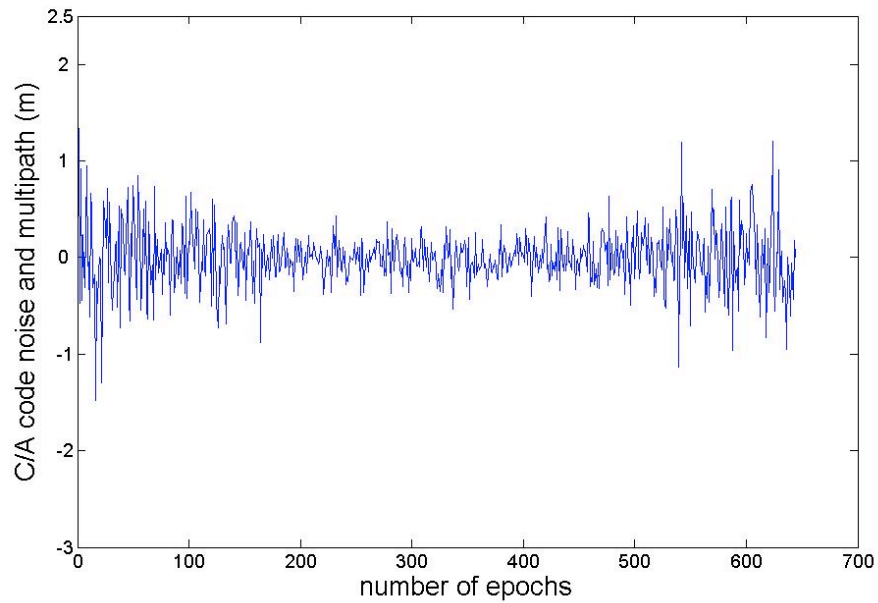


Figure 5.4 Noise and multipath level of C/A– PRN 11

Table 5.2 Standard deviations of P2 and C/A-code noise and multipath - PRN 11

	Standard deviation (m)
P2	0.438
C/A	0.315

The computed standard deviations of C/A and L2C code multipath and noise levels for PRN 17 are summarized in Table 5.1. According to Simsky et al. (2006), the same level of noise and multipath is expected on C/A and L2C.

Our results show a contrast with this assumption as the standard deviation of the noise level of L2C signal is 0.611 m, while it is 0.270 m for the C/A code. Therefore, according to our results, the noise level of the L2C code is higher than the noise of the C/A code. Why is there a contrast between the assumption of same multipath and noise level and the obtained results? An explanation for the higher noise and multipath on the

L2C code is in the firmware of the Trimble R7 receiver used during the data collection (v. 2.26 and v. 2.28). The main reason why there were differences in noise level is that Everest (Trimble's multipath mitigation algorithm) was not enabled on L2C. As pointed out by Mallen (2007) there were also some residual tracking issues which slightly increased the noise on the L2C observable. The differences seen in noise level therefore came mainly from the different treatment given to the observations, rather than purely tracking problems. Both issues were fixed in firmware version 2.30 which was released on 21 September 2006. However the data for the analyses presented in this report were collected prior to the release of the new firmware version 2.30. Tests are currently underway to assess the performance of this new firmware version.

Table 5.2 summarizes the multipath and noise level of C/A and P2 codes of PRN 11. The standard deviations of the multipath and noise levels of P2 and C/A codes are 0.438 m and 0.315 m, respectively.

If we compare Figure 5.3 to Figures 5.1, 5.2 and 5.4 we can see that the P2 code performance at low elevation angles on the multipath and noise is different from that of the other codes. This trend can be explained by the firmware issues which, according to the manufacturer, have been fixed in v.2.30 (Mallen, 2007).

Conclusions

The L2C modernized civil signal has been collected at UNB from 11 January 2006 until 10 October 2006 using a Trimble R7 receiver. After the observation and navigation files have been created several analyses were made on the L2C signal. First, the signal-to-noise ratios of all satellites were compared on the L1 and L2 frequencies. The conclusion from the comparison is that the signal-to-noise ratio of L2C signal is higher than the signal-to-noise ratio of P2 code, and reaches a similar value as that of the SNR of the C/A code on the L1 frequency.

In the next step, the noise level of the L2C and C/A code was calculated and analyzed. From the comparison of the multipath and noise of the two codes it can be seen that the noise level of the L2C code was higher than the noise of the C/A code. This fact contradicts the expectation of having similar noise and multipath levels for both L2C and C/A code. However this can be explained by issues in the firmware versions 2.26 and 2.28, which were used in the Trimble R7 receiver during the observation period. Those issues have been fixed in the new firmware release, version 2.30 (Mallen, 2007). A new set of tests is underway to assess the performance of the R7 receiver in operation under this new firmware and will be presented in a subsequent report.

Acknowledgments

We gratefully acknowledge Cansel Ltd for the loan of the Trimble R7 receiver used in this study and Trimble Canada Ltd. for helpful discussions. We would also acknowledge the GEOIDE Network of Centres of Excellence for funding of our work. This research has been developed under the GEOIDE project “Next-generation algorithms for navigation, geodesy and earth sciences under modernized Global Navigation Satellite Systems (GNSS)”.

References

- Langley, R.B. (1998). *GPS for Geodesy*. 2nd Edition (P.J.G Teunissen and A. Kleusberg, Editors), Springer-Verlag, Berlin, Heidelberg, and New York, 650 pp.
- Langley, R.B. (2006). IGSMail-5406: UNB1 Decommissioned; UNBJ Established. [On-line] Retrieved 10 September 2006 from IGSMail, igsbc.jpl.nasa.gov, <http://igsbc.jpl.nasa.gov/mail/igsmail/2006/msg00129.html>
- Mallen, B. (2007). Personal Communication. Trimble Canada Ltd., Toronto, Ontario, Canada.
- Simsky, A., J.M. Sleewaegen, P. Nemry, and J.V. Hees (2006). "Signal performance and measurement noise assessment of the first L2C signal-in-space." Proceedings of Position, Location, And Navigation Symposium, 2006 IEEE/ION, San Diego, California, 24-27 April, pp. 834- 839.
- Space Environment Center (2006). Estimated Planetary K Index (3 Hour Data) http://www.sec.noaa.gov/ftplib/warehouse/2006/2006_plots/kp.tar.gz, Web site accessed 10 July 2006.